

1 **Biomass-derived carbon dots as emerging visual platforms**
2 **for fluorescent sensing**

3 *Lili Yuan^a, Congying Shao^{a*}, Qian Zhang^a, Erin Webb^b, Xianhui Zhao^{b*}, Shun Lu^{c*}*

4 a Key Laboratory of Green and Precise Synthetic Chemistry and Applications, Ministry of
5 Education, School of Chemistry and Materials Science, Huaibei Normal University, Huaibei,
6 Anhui 235000, China

7 b Environmental Sciences Division, Oak Ridge National Laboratory, Oak Ridge, TN 37830,
8 United States

9 c Chongqing Institute of Green and Intelligent Technology, Chinese Academy of Sciences,
10 Chongqing 400714, China

11 * Corresponding authors

12 Email addresses: shaocongying@163.com (C. Shao), zhaox@ornl.gov (X. Zhao),
13 lushun@cigit.ac.cn (S. Lu)

14

15 **Abstract:**

16 Biomass-derived carbon dots (CDs) are non-toxic and fluorescently stable, making them
17 suitable for extensive application in fluorescence sensing. The use of cheap and renewable
18 materials not only improves the utilization rate of waste resources, but it is also drawing
19 increasing attention to and interest in the production of biomass-derived CDs. Visual
20 fluorescence detection based on CDs is the focus of current research. This method offers high
21 sensitivity and accuracy and can be used for rapid and accurate determination under complex

22 conditions. This paper describes the biomass precursors of CDs, including plants, animals and
23 microorganisms. The factors affecting the use of CDs as fluorescent probes are also discussed,
24 and a brief overview of enhancements made to the preparation process of CDs is provided. In
25 addition, the application prospects and challenges related to biomass-derived CDs are
26 demonstrated.

27 **Keywords:** Biomass conversion, carbon dots, visual platforms, fluorescent probe, fluorescent
28 mechanisms

29

30

31

32

33

34

35

36

37

38

39

40

41 **1. Introduction**

42 The fluorescence sensor is a compound that contains a binding site, a
43 fluorophore, and a communication mechanism between two sites
44 (Brzechwa-Chodzyńska et al., 2021). The mechanism of detection is a probe that
45 detects the object based on changes in optical properties. These sensors boast high
46 sensitivity and accuracy, and they have broad application prospects in food analysis
47 (Liu et al., 2019b; Luo et al., 2020; Pan et al., 2020), metal ions detection (Mehta et
48 al., 2021; Yang et al., 2020) and other fields (Shin et al., 2021). Furthermore, research
49 in the area of fluorescence sensor development targets cheap and simple structure
50 (Zhang et al., 2023a). Traditional detection methods rely primarily on fluorescence
51 spectrometers. However, this approach requires equipment and professional
52 personnel, and the cost is higher. However, fluorescent sensing can be designed as an
53 emerging visualization platform. The visualization method is accomplished with the
54 help of simple, inexpensive instruments, such as the use of test strips or smartphone
55 apps to facilitate testing (Castro et al., 2021). The advantage is that the reagent
56 consumption is low, and such devices can be easy to carry. Yu et al., for example,
57 used a portable fluorescent device for field detection. In their approach, the
58 fluorescence signal is captured by a smartphone camera and converted into an image,
59 and quantitative analysis is completed by the red, green, and blue (RGB) value of the
60 image (Liang et al., 2022). Fluorescent sensors have been widely used, but there is

61 still room for further development in biomedical (Chen et al., 2021; Duo et al., 2023)
62 or microenvironment monitoring (Shin et al., 2021; Yin et al., 2021). To improve the
63 detection efficiency of fluorescence sensors, the method of coupling
64 high-performance materials (De Acha et al., 2019) or absorptive fluorescence
65 modulation of solid surface can be employed (Yang et al., 2014).

66 Carbon dots (CDs) are carbon-based zero-dimensional materials with good
67 photostability and biocompatibility (Meng et al., 2019). CDs have important
68 applications in fluorescence sensing, various optical devices (Castelletto and Boretti,
69 2023; Li et al., 2023c), electrode materials (Niyitanga et al., 2023), and room
70 temperature phosphorescent materials (Hu et al., 2023; Li et al., 2023b). CDs are a
71 kind of carbon hybrid nanomaterial, mainly composed of carbon quantum dots
72 (CQDs) (Rasal et al., 2021), graphene quantum dots (GQDs) (Biswas et al., 2021),
73 and carbonized polymer dots (CPDs) (Kang et al., 2022). GQDs consist of one or
74 more layers of graphene whose edges are connected by chemical groups (Ai et al.,
75 2021). CPDs are crosslinked polymer or polymer chains based on monomers or linear
76 polymers (Ai et al., 2021). CQDs have a graphite lattice structure with distinct lattice
77 fringes (Ai et al., 2021; Innocenzi and Stagi, 2023). GQD precursors are essentially
78 graphitized, such as graphite, carbon nanotubes, etc., whereas CQDs are composed of
79 carbon-rich precursors, and there are more kinds of precursors for CQDs (Deka et al.,
80 2022). A variety of raw materials are used in the preparation of carbon materials,
81 including graphite, small molecules, polymers, and natural materials (Xia et al.,
82 2019). Among these, biomass materials are rich in carbon and a variety of other

83 elements (Abbas et al., 2018; Wang et al., 2021b), and preparing carbon materials as
84 precursors can reduce the use of chemical reagents. Biomass materials include plants,
85 animals, microorganisms, and so on. Plants are popular precursors for the preparation
86 of carbon materials and are rich in cellulose, hemicellulose, and lignin (Wang et al.,
87 2021b). Animal bone and animal protein can also be used as precursors for carbon
88 materials, and their derived materials contain amino acids, proteins and trace elements
89 (Fan et al., 2022). The processing methods of biomass conversion into carbon
90 materials include hydrothermal carbonization, pyrolysis, microwave radiation,
91 catalytic conversion, etc. (Malode et al., 2023a; Wang et al., 2021b).

92 The production of carbon materials from biomass materials not only improves
93 the utilization rate of waste materials, but it also reduces the cost of carbon material
94 preparation. For the disposal of waste, the incineration or random placement of
95 agricultural waste and residues can cause environmental pollution problems (Abbas et
96 al., 2018). By using renewable, cheap biomass as a carbon source, we can both
97 maximize the use of energy and create new avenues for energy utilization. Biomass
98 material as a precursor makes green synthesis simpler, and the material comes from a
99 wide range of sources, doped by a variety of atoms (Fan et al., 2022). Biomass
100 derived CDs offer low cost, low toxicity and environmental friendliness, and they can
101 be used for large-scale preparation and biomedicine. Compared with non-biomass
102 CDs, the heteroatoms in biomass can achieve self-doping, which gives the CDs
103 excellent properties (Fang et al., 2024). In addition, compared to other fluorescent
104 probes, such as organic dyes (rhodamine, cubic acid), semiconductor quantum dots,

105 and precious metal nanoclusters, biomass derived CDs do not contain heavy metal
106 elements and have good biocompatibility. Moreover, these CDs have the advantages
107 of low cost, good light stability, strong photobleaching resistance, and good water
108 solubility (Li et al., 2021d; Liu et al., 2024; Mathew and Mathew, 2023b; Zhang et al.,
109 2022b).

110 Previous research efforts have discussed the synthetic and fluorescent properties
111 of CDs, as well as their applications in food analysis and detection of metal ions (Li et
112 al., 2023a; Yoo et al., 2019). Biomass CDs are also mainly focused on synthetic
113 pathways, fluorescence mechanisms, and application (Jing et al., 2023; Liu et al.,
114 2019a). However, the significance and innovation of this research are focusing on the
115 influencing factors and improvement of fluorescence sensing. The detection
116 mechanisms are summarized, and the improvement of biomass-derived CD
117 preparation is provided. The effects of pH, temperature, reaction time, and reactant
118 ratio on the application of CDs are studied. Moreover, the optimization of reaction
119 conditions, the use of sustainable carbon sources, and element doping are briefly
120 discussed. In addition, the precursors of biomass-derived CDs are briefly described
121 and summarized. Finally, the prospects and challenges related to biomass-derived
122 CDs are presented (**Fig. 1**).

123

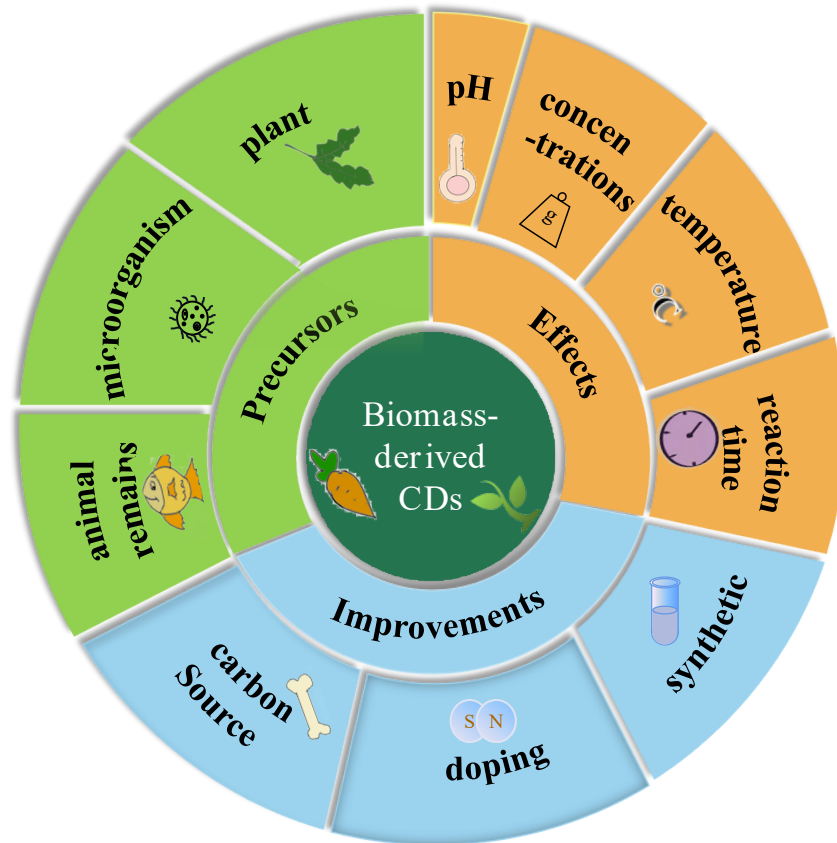


Figure 1. Precursors, effects, and improvements of biomass-derived CDs.

2. Mechanisms of fluorescent sensors

2.1 Aggregation-induced emission mechanism

Fluorescence sensing has the advantages of good sensitivity, fast response speed, and low cost. When the concentration of the analyte changes the fluorescence properties, the system can be considered for sensing (Deka et al., 2022). Various mechanisms have been proposed to explain fluorescence sensing (Table 1). Aggregation-induced emission (AIE) is a general strategy designed for sensing

134 systems. The fluorophores induced by fluorescence aggregation have the advantages
135 of high emission efficiency, strong light stability, and large Stokes shifts. The study
136 mechanism of AIE includes restriction of intramolecular motion, excimer formation,
137 polymerization, etc. Of these, the restriction of intramolecular motion may
138 specifically refer to constraints on intramolecular rotation and vibration (Gao and
139 Tang, 2017). Many luminous materials display AIE properties and can be pure
140 hydrocarbons, organometallic molecules, polymers, and so on (He et al., 2018). For
141 CDs, the chemical stability as well as the tunable and up-photoluminescence behavior
142 of CDs offer great potential in the application of fluorescence sensors (Liang et al.,
143 2022; Salimi Shahraki et al., 2022). AIE phenomena were shown to occur in CDs
144 prepared by Yang et al., in which Polyethylenimine (PEI) and citric acid were used as
145 raw materials for the preparation of CDs. After adenosine triphosphate (ATP) was
146 added, the fluorescence intensity and quantum yield of CDs were enhanced. The AIE
147 phenomenon was determined to be a result of the coordination and electrostatic
148 interaction between ATP and prepared CDs. Based on the AIE phenomenon, a simple
149 ATP detection platform was established (Huang et al., 2022b). In addition, the
150 literatures on materials detection based on the mechanism of AIE is extensive (Li et
151 al., 2021b; Zhang et al., 2023b). Substances with AIE characteristics have significant
152 application prospects in sensing and bioimaging (Niu et al., 2020), as well as in
153 medical (Gao and Tang, 2020) and other fields. However, when they are applied in
154 complex environments, more stringent requirements are imposed with respect to
155 specificity and sensitivity (Wang et al., 2023b). Achieve these two requirements is a

156 challenge in the process of material exploration.

157

158 **Table 1.** Applications of CDs under different mechanism types.

Mechanisms	CDs	Detector	Read Out	Linear range	LOD	Ref.
AIE	Nitrogen-doped CDs	ATP	Turn-on	1–2000 μM	0.8 μM	(Huang et al., 2022b)
	Red fluorescent CDs	Tetracycline antibiotics	Turn-on	3–35 μM (TC)	12 nM (TC)	(Li et al., 2021b)
	Tea saponin-CDs	Human serum albumin	Turn-on	0–180 μM	140 nM	(Zhang et al., 2023b)
Static quenching	Nitrogen-doped CDs	Curcumin	Turn-off	0.1–20 μM	29.8 nM	(Tang et al., 2021a)
	CDs	Sunset yellow	Turn-off	0.3–56 $\mu\text{mol L}^{-1}$	74 nmol L^{-1}	(Yang et al., 2018)

Dynamic quenching	O-CDs	Morin; ClO ⁻	Turn-off	5–125 μM (morin); 2.5-90 μM (ClO ⁻)	0.8 μM; 0.5 μM	(Meng et al., 2022)
	Nitrogen-doped grape peels CDs	Baicalin	Turn-off	0.1-20 μM	43.8 nM	(Tang et al., 2022)
	N,S-BCDs	Cr (VI)	Turn-off	0-400 μM	0.2 μM	(Wang et al., 2022a)
	N-CDs (citric acid+benzoylurea)	Fe(III)	Turn-off	30-100 μM	1.1 μM	(Shan et al., 2021)
FRET	N-CDs	p-nitrophenol	Turn-off	0.5-70 μM	0.2 μM	(Liao et al., 2021a)
	CD	Oxytetracycline	Turn-on	0-40 μM	0.4 μM	(Fu et al., 2021)
	CDs	Dithizone	Turn-off	—	—	(Liu et al., 2020)
IFE	CDs-MnO ₂ nanosheets	Dopamine	Turn-on (elimination of IFE)	1-30 μM	100 nM	(Tan et al., 2020b)

N-CDs	MnO ₄ ⁻	Turn-on	0.2-9.0 μM	0.1 μM	(Chen et al., 2022a)
CNF-TCDs3	Cr(VI)	Turn-off	0-15 mg/L	0.2 mg/L	(Hu et al., 2022)

159

160 2.2 Static quenching mechanism

161 Various fluorescence changes (e.g., intensity, wavelength, lifetime) of CDs are
 162 relevant to their potential as sensors, and these changes are also related to the
 163 fluorescence sensing mechanism (Sun and Lei, 2017). Static quenching is the
 164 interaction of probe and quencher to form a non-fluorescent ground state complex
 165 (Liu et al., 2019a). Fluorescence quenching occurs when CDs are used as probes to
 166 detect substances, and the possibility of static quenching should be considered. The
 167 nitrogen-doped fluorescent CDs (NCDs) prepared by Yu et al. can be used to detect
 168 curcumin, and the mechanism of detection involves static quenching and internal
 169 filtration effects (Tang et al., 2021a). The fluorescence lifetime of NCDs did not
 170 change significantly after curcumin was added, and the quenching type was
 171 determined by using the standard Stern-Volmer equation. In addition, Hu et al.
 172 prepared CDs via a hydrothermal process, which can be used to detect sunset yellow
 173 (Yang et al., 2018). The quenching mechanism is also studied with the help of the
 174 Stern-Volmer equation $F_0/F = 1 + K_q\tau_0[Q] = 1+K_{sv}[Q]$. Here, K_q is the quenching

175 constant, and K_{sv} is the Stern-Volmer quenching constant. F and F_0 are the
176 fluorescence intensity of CDs before and after adding sunset yellow, τ_0 is the
177 fluorescence lifetime before adding quencher, and $[Q]$ is the concentration of adding
178 quencher. Static quenching can be distinguished according to the change of the
179 quenching constant at different temperatures. In this system, the quenching constant
180 decreases with the increase in temperature, which confirms that the mechanism is
181 static quenching. The fluorescence lifetime did not change significantly before and
182 after adding sunset yellow, which further proves that the quenching mechanism is
183 static quenching.

184

185 **2.3 Other mechanisms**

186 According to the fluorescence quenching phenomenon, the mechanism of the
187 analyte detection includes dynamic quenching (Zu et al., 2017), Forster resonance
188 energy transfer (FRET), inner filter effect (IFE), and so on (**Fig. 2**). FRET is a
189 non-radiative energy transfer process between donor-acceptor pairs (Wu et al., 2020).
190 IFE refers to the effect in which the observed fluorescence intensity in a system is
191 proportional to the intensity of the excited light, and the quantum yield is slightly
192 lower than that of infinite dilution (Chen et al., 2018; Li and Zhang, 2021; Li et al.,
193 2021d). IFE production may be caused by concentration effects or by the capture of
194 the excited light by the absorbent and the emitted light of the fluorophores, resulting
195 in reduced fluorescence (Li and Zhang, 2021). The practical application of CDs
196 cannot be separated from the support of fluorescence sensing theory. The fluorescence

197 mechanism of CDs can be explained by molecular state, surface state, size, and other
 198 theories. As the degree of CDs carbonization increases, core-shell structure is
 199 gradually formed. The fluorescence mechanism of CDs in the formation of core-shell
 200 structures is the most widely studied (Wang and Lu, 2022). The application of CDs is
 201 based on changes in fluorescence caused by the interaction of the analyte with CDs
 202 (Zu et al., 2017). In addition, CDs as a probe can also be used to detect molecules and
 203 anions, as shown in **Table 2**. Moreover, carbon material-based fluorescence sensors
 204 have been shown to effectively detect targets in organisms and the environment, using
 205 bioimaging technology or combined with smartphones to achieve real-time
 206 monitoring of targets (Li et al., 2023a). FRET, IFE, and static quenching mechanisms
 207 have been widely used in detection using CDs as fluorescent probes (Wang and Lu,
 208 2022). AIE uses a turn-on model to analyze species, while AIE luminogens has low
 209 background noise and good light stability (Wang et al., 2023a).

210

211 **Table 2.** Detecting anions and molecules by fluorescence detection mechanism.

	Detector	CDs	Mechanism	Ref.
Anion	ClO^-	N-CQDs	Dynamic quenching	(Jiang et al., 2020)
	MnO_4^-	N-CDs	Inner filter effect	(Chen et al.,

				2022b)
	ClO^-	N,Cl-CDs	Dynamic quenching; photoinduced electron transfer	(Liu et al., 2021b)
	S^{2-}	N, S-CDs	High affinity between S^{2-} and Sn^{2+}	(Liao et al., 2023)
	PO_4^{3-}	GQDs	Strong affinity between PO_4^{3-} and $\text{Ce}^{4+}/\text{Fe}^{3+}$	(Wang et al., 2022b)
	Adenosine triphosphate	Nitrogen-doped CDs	Aggregation-induced emission	(Huang et al., 2022a)
Molecule	Curcumin	Nitrogen-doped CDs	Static quenching	(Tang et al., 2021b)
	Tetracycline antibiotics	Red fluorescent CDs	Aggregation-induced emission	(Li et al., 2021c)

			(Liao
p-nitrophenol	N-CDs	Forster resonance energy transfer	et al.,
			2021b)
			(Tan et
Dopamine	CDs-MnO ₂ nanosheets	Inner filter effect	al.,
			2020a)

212

213 The mechanism by which CDs are applied to fluorescence sensing is described
214 above. As fluorescent probes, CDs can be used to detect molecules (thiols, antibiotics,
215 nitroaromatics, proteins), ions (Fe³⁺, Hg²⁺, Cu²⁺, S₂O₃²⁻, ClO⁻, PO₄³⁻), pH, temperature
216 and so on. Biomass CDs have good response to a variety of substances and can be
217 used for the detection and analysis of actual samples (Liu et al., 2019a; Malode et al.,
218 2023a). In industrial engineering, biomedical monitoring and environmental control,
219 temperature and pH measurements are the basis for ensuring efficient and reliable
220 operation of the system in question. As substances that are sensitive to temperature
221 and pH, CDs have great research value (Yadav et al., 2023; Zhang et al., 2019).

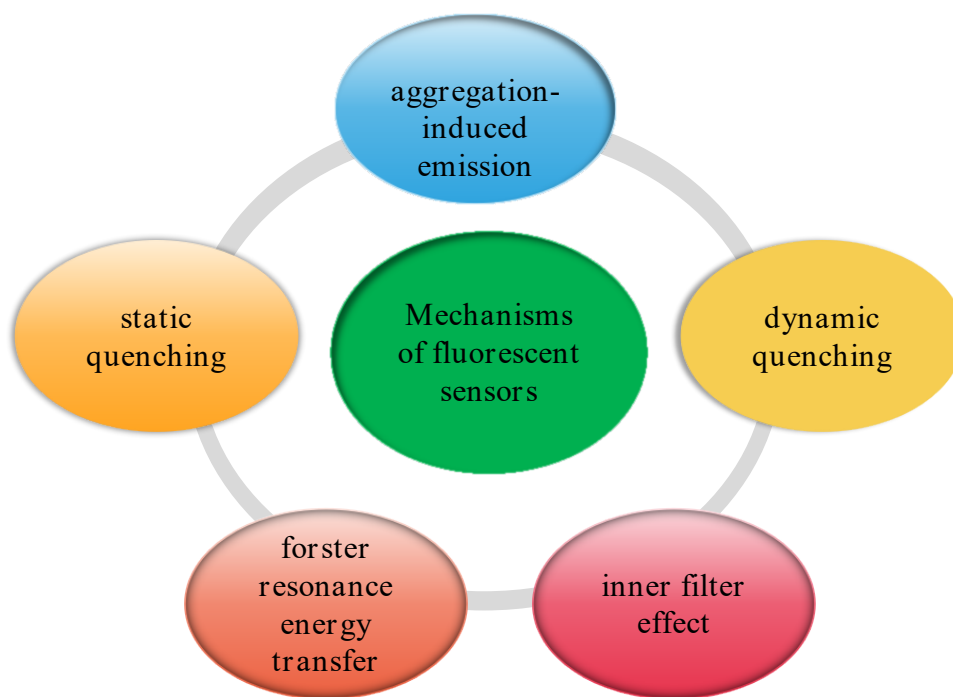


Figure 2. Mechanisms of fluorescent sensors

222

223

224

225 **3. Precursors in biomass-derived carbon dots**

226 **3.1 Structure and preparation of carbon dots**

227 The analysis of CDs structure is challenging because CDs vary in size and
 228 optical properties, which complicates the interpretation of structural data. In addition,
 229 determining whether the captured signal comes from the surface or the core is a
 230 problem (Mintz et al., 2021). The crystal properties of CDs can be further studied by
 231 high-resolution transmission electron microscopy (HRTEM), X-ray diffraction
 232 (XRD), and other techniques (Liu et al., 2019a). CDs synthesis involves breaking

233 apart chunks of material or assembling atoms or molecules to form nano-sized
234 particles (Kumar et al., 2022). CDs can be prepared by hydrothermal synthesis
235 (Perumal et al., 2021), microwave-assisted synthesis (Ng et al., 2021), chemical
236 oxidation (Meng et al., 2019), ultrasonic synthesis, among other techniques. The
237 hydrothermal method can use a variety of biomass materials as a carbon source,
238 which has the advantages of environmental protection and low cost (Perumal et al.,
239 2021). Microwave-assisted synthesis can shorten the hydrothermal time, but the
240 quantum yield cannot be improved significantly (Ng et al., 2021). Chemical oxidation
241 can use strong oxidizing acids to carbonize organic matter; however, the harmful
242 effects of strong oxidizing acids on the environment limit the application of this
243 method (Jing et al., 2023). The method of obtaining raw materials from nature to
244 prepare CDs is green and pollution-free, and the reuse of waste materials (e.g., peel,
245 bone) also addresses the problem of household waste disposal.

246 Common synthesis methods of biomass derived CDs include hydrothermal
247 method, electrochemical oxidation, chemical oxidation, microwave, and pyrolysis. To
248 improve the fabrication of biomass-derived CDs, ball mill can be used to treat the
249 material in the raw material pretreatment process, and the consistent particle size can
250 be tuned by controlling the parameters. To make biomass derived CDs with special
251 functions, carbon sources with special structures can be selected. It is also possible to
252 change the morphology or properties of CDs by changing reaction solvents, or to
253 change the optical and electronic properties via element doping. For the reaction
254 solvent, its dewatering ability, polarity, and proton properties all affect the properties

255 of CDs (Gan et al., 2023; He et al., 2023; Malode et al., 2023b; Mathew and Mathew,
256 2023a; Miao et al., 2020; Rasheed, 2023).

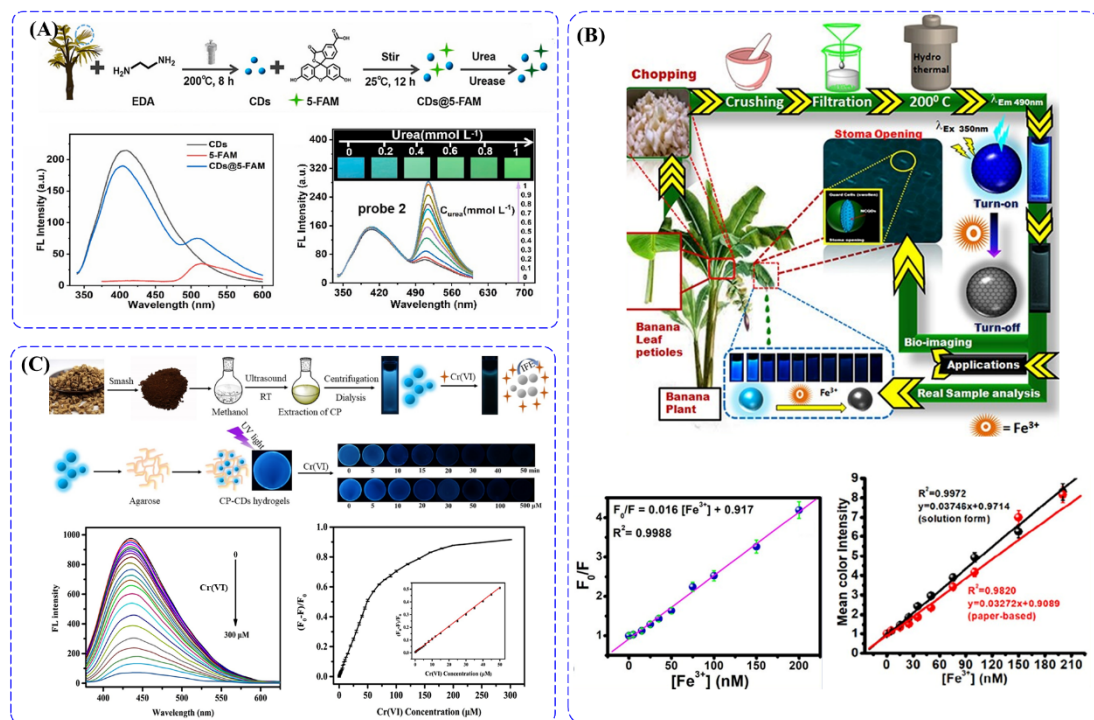
257

258 **3.2 Plant-based biomass**

259 In the process of CDs synthesis, biomass materials are selected as carbon
260 precursors, which are advantageous because they are non-toxic and low cost (Cao et
261 al., 2022b; Deng et al., 2021; Feng et al., 2021). Both plant and animal remains can be
262 used as materials to synthesize CDs (**Table 3**). Likewise, plant residues have great
263 potential in the synthesis of CDs (Arumugham et al., 2020; Gupta et al., 2020; Li et
264 al., 2018; Shen et al., 2017). Shang et al. prepared CDs by a hydrothermal method
265 using *Toona sinensis* leaves and ethylenediamine (EDA) as raw materials (Bei et al.,
266 2023). To improve the sensitivity, a ratio fluorescence probe (CDs@5-FAM) was
267 constructed using CDs and 5-carboxyfluorescein (5-FAM). In this method, as the
268 concentration of urea increases, the fluorescence changes from blue to green under
269 UV light (**Fig. 3A**). Sawant et al. for the first-time prepared biomass-derived CDs
270 using banana petioles as precursors. The CDs can be used as a sensing probe for Fe³⁺
271 detection with a detection limit of 0.21 nM. The detection mechanism is photoinduced
272 electron transfer to form a non-radiative charge transfer complex. In addition, solution
273 and paper-based analysis methods were designed based on smart phones. The
274 relationship between the average color intensity and iron concentration was obtained
275 by analyzing the image with software (Korram et al., 2023). (**Fig. 3B**).

276 Furthermore, Fu et al. obtained high fluorescence CP-CDs from rice fried

277 Codonopsis pilosula (CP) by ultrasonic-assisted solvent extraction at room
 278 temperature (Qiu et al., 2020). CP-CD production process was simple, convenient,
 279 and green. CP-CDs showed high light stability and could be used for the detection of
 280 Cr (VI) in environmental sewage samples. CP is a common Chinese medicine.
 281 Therefore, making CP-CDs with CP reduces the cost of synthesis and expands the
 282 application value of traditional Chinese medicine resources (Fig. 3C).



283
 284 **Figure 3.** (A) The preparation process and fluorescence spectra of CDs@5-FAM, and the effect of
 285 increasing urea concentration on probe fluorescence spectrum. Reprinted with permission from Ref.
 286 (Bei et al., 2023). Copyright 2022, Elsevier. (B) Synthesis and fluorescence response of probe and
 287 construction of fluorescence sensing platform of smart phone. Reprinted with permission from Ref.
 288 (Korram et al., 2023). Copyright 2023, American Chemical Society. (C) Preparation of CP-CDs and
 289 detection of Cr (VI). Reprinted with permission from Ref. (Qiu et al., 2020). Copyright 2020, Elsevier.

291 **Table 3.** Summary of precursors in biomass-derived carbon dots.

Carbon precursor	Quantum yield (%)	Size (nm)	Detector	Linear range	LOD	Recovery (%)	Ref.
Toona sinensis leaves	17	2.5	Urea	—	0.014 mmol·L ⁻¹ (CDs@5-FAM)	93	(Bei et al., 2023)
Andrographis paniculata	98.6–101.1; 97.6–103.4 (fluorescence spectrum)	170	Cu(II); L-cysteine	0.1–200 μM; 5–100 μM	71 nM; 12 nM (fluorescence spectrum)	98.2–101.6; 103.3–121.6 smartphone-integrated optosensors	(Zhang et al., 2022a)
Banana petioles	8.5	3.3	Fe ³⁺	5–200 nM	0.21 nM	98.7–105.4	(Korram et al., 2023)
Rice fried Codonopsis pilosula	12.8	9.60 (methanol), 11.54 (aqueous solution)	Cr (VI)	0.03–50 μM	15 nM	94.6–107.8	(Qiu et al., 2020)
Escherichia coli BW25113	15.8	2.9	p-NP, microbial cells	—	11 nM (p-NP)	—	(Qin et al., 2019)

CFS of <i>L. acidophilus</i>	—	2.8	Antimicrobial/ultra violet protective bacterial nanocellulose film	—	—	—	(Koush et al., 2020)
Chitosan	35	2.8	NO_2^-	1–500 μM	0.1 μM	—	(Sun et al., 2021)
Animal bones	—	6.7 (PBCDs); 6.6 (BBCDs); 9.5 (SBCDs)	Ag^+ , Cu^{2+} , Hg^{2+} , Fe^{3+} , Pb^{2+}	—	—	—	(Fu et al., 2022)
Pork rib bones	—	4.2	Dimethoate	0.15–5.0 μM	0.064 μM	93–105	(Liu et al., 2020)
Cow milk	38	7	Sn^{2+}	—	17 μM	—	(Kumar et al., 2022)

292

293 3.3 Microorganism-based biomass

294 A variety of biomass materials have been used for carbon source research and
 295 exploration, including microbial materials. Carbon-containing substances can be
 296 obtained from microbial biomass, which provides raw materials for CDs preparation.
 297 Microbial cells are rich in organic compounds, including proteins containing N, S,
 298 and other heteroatoms, which are ideal materials for constructing CDs
 299 (Oladzadabbasabadi et al., 2023). Wei et al. prepared CDs using *Escherichia coli*

300 BW25113 (WT) as a carbon source, which can be used for microbial imaging and
301 p-nitrophenol (p-NP) detection (Qin et al., 2019). It has good biocompatibility and
302 can be excreted quickly through the intestine, which also proves that CDs have the
303 characteristics of low toxicity. CDs can also be used as fluorescent probes for the
304 selective detection of p-NP, and the monitoring mechanism is the internal filtration
305 effect (**Fig. 4A**). Moradi et al. synthesized CDs with antibacterial activity from
306 cell-free supernatant (CFS) of lactobacillus acidophilus (Kousheh et al., 2020). CDs
307 were introduced into bacterial nanocellulose membranes, and functional nano-papers
308 with anti-microbial/UV blocking capabilities were also prepared. The work by Moradi
309 et al. was the first to apply the CFS of probiotics to CDs production. Xiong et al. used
310 chitosan derived CDs for NO_2^- determination and bacterial imaging (Sun et al., 2021).
311 Chitosan is a linear poly cationic biopolymer (Zhang et al., 2023c). The fluorescence
312 of N-doped carbon dots (N-CDs) can be selectively quenched due to static quenching
313 and internal filtration effect. Based on this finding, a fluorescence sensor can be
314 designed to complete the measurement in a real sample. The prepared CDs have low
315 toxicity to bacteria and can stain bacterial cells through cell membranes or cell walls,
316 making them a good choice for biological imaging (**Fig. 4B**).

331 Animal remains can also be explored as carbon sources, including bones (Fu et
332 al., 2022; Liu et al., 2020), cow manure (Horst et al., 2021), fish scale (Dhandapani et
333 al., 2020), and silkworm cocoons (Wang et al., 2020). The value of bone as kitchen
334 waste is low, and the transformation into CDs improves its application value and
335 realizes the reuse of waste resources. Chen et al. prepared pork bone BCDs (PBCDs),
336 bovine bone BCDs (BBCDs), and sheep bone BCDs (SBCDs) via a hydrothermal
337 method using different raw materials to distinguish heavy metal ions (Ag^+ , Cu^{2+} ,
338 Hg^{2+} , Fe^{3+} , Pb^{2+}) (Fu et al., 2022). Due to the different content of elements in the three
339 CDs, different affinities for metal ions led to different degrees of quenching (**Fig. 4C**).
340 Ding et al. prepared CDs by treating pork rib bones in a simple way, which was cheap
341 to manufacture and easy to operate (Liu et al., 2020). On this basis, the fluorescence
342 switching process was also established. Dithizone was shown to quench the
343 fluorescence of CDs, and the addition of dimethoate restored the fluorescence.
344 Dithizone-functionalized CDs could be used for the detection of organophosphorus
345 pesticide dimethoate, which was of great significance for the protection of the
346 ecosystem (**Fig. 4D**). In addition to animal bones, CDs could also be created from
347 cow milk through a simple hydrothermal synthesis process (Kumar et al., 2022). CDs
348 can also selectively detect Sn^{2+} through a fluorescence quenching mechanism, which
349 is an optional method to detect Sn^{2+} in the environment. What's more, CDs are stable
350 under UV irradiation and high salt conditions, which also shows that they can be used
351 in practical situations (**Fig. 4E**). The quantum yield of animal-derived CDs is lower
352 than that of plant waste-derived CDs (de Oliveira and da Silva Abreu, 2021).

353 However, the animal material contains rich chitin and protein contents, and it contains
354 rich C, O, N elements. N-containing groups give CDs special properties, such as those
355 related to fluorescence (Kuang et al., 2023).

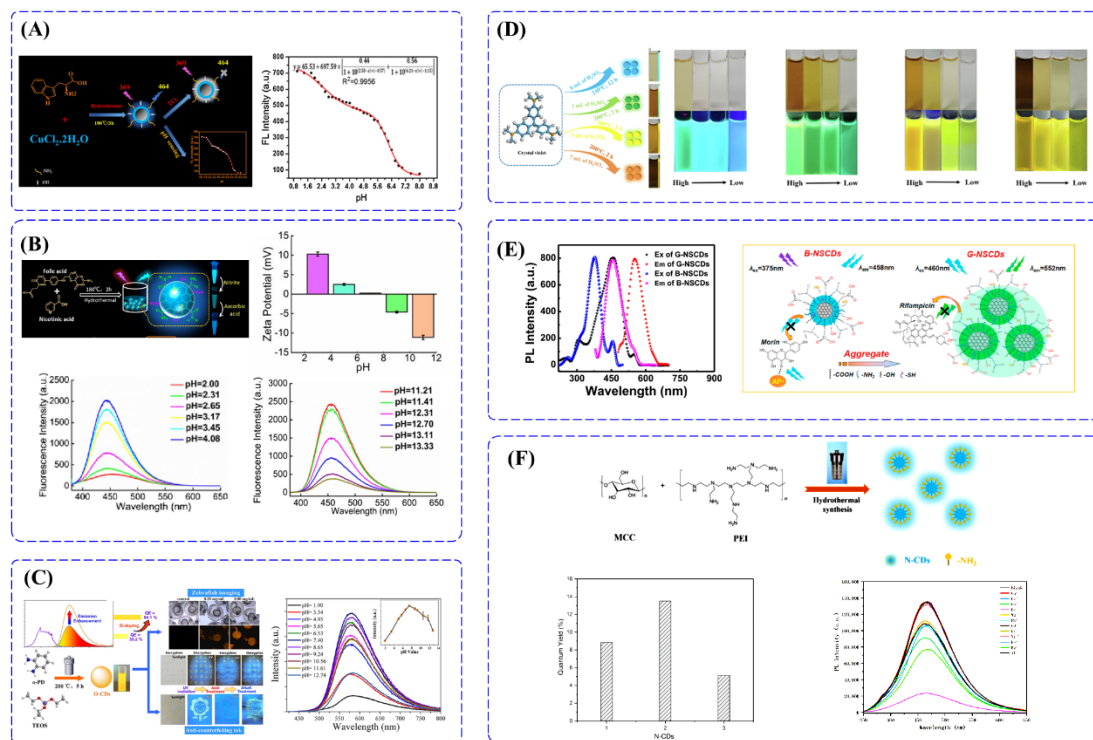
356

357 **4. Effects of carbon dots for fluorescent sensing**

358 **4.1 pH**

359 As previously stated, many factors affect the fluorescence color and intensity of
360 CDs, such as pH (Das et al., 2020; Meierhofer et al., 2020), reactant ratio, temperature,
361 and time of synthesis. Copper-doped fluorescent carbon dots (Cu-CDs) with blue
362 fluorescence were prepared by Shuang et al. (Guo et al., 2021). Under acidic
363 conditions, the fluorescence intensity decreases with the increase of pH value, which
364 can be used to detect the change of intracellular pH value. Introducing the pH
365 response of Cu-CDs into the study of fluorescent probes will further expand its
366 application field (**Fig. 5A**). In addition, CDs prepared by Chen et al. with folic acid
367 and nicotinic acid has a high sensitivity to pH, which is expected to be used for pH
368 sensing (Gan et al., 2020). Using the change of zeta potentials, the protonation and
369 deprotonation of CD surface functional groups were investigated to clarify the
370 response of CDs in an acid-base environment (**Fig. 5B**). Zhang et al. synthesized
371 orange luminescent carbon dots (O-CDs) using o-phenylenediamine and ethyl
372 orthosilicate as raw materials using a hydrothermal method (Sun et al., 2022). O-CDs
373 can be used as fluorescent ink to encrypt data. The fluorescence intensity is highest
374 under neutral conditions. The surface functional groups undergo protonation and

375 deprotonation under acidic and alkaline conditions, with obvious fluorescence
 376 quenching. By utilizing the characteristics of O-CDs, anticounterfeiting ink is
 377 designed to be written on paper and then sprayed with hydrochloric acid to complete
 378 the encryption of information. Fluorescence is quenched by acid but can be restored
 379 by an alkaline solution. The O-CDs have potential application value in encrypted data
 380 and anticounterfeiting applications (Fig. 5C).



381
 382 **Figure 5.** (A) The synthesis route of Cu-CDs and the fitting curve of relative fluorescence attenuation
 383 and pH. Reprinted with permission from Ref. (Guo et al., 2021). Copyright 2020, Elsevier. (B) CD
 384 composite diagram, CD correlation spectrum and zeta potentials at different pH levels. Reprinted with
 385 permission from Ref. (Gan et al., 2020). Copyright 2020, Elsevier. (C) The synthesis scheme of O-CDs
 386 and their application, as well as the luminescence spectra of O-CDs under different pH conditions.
 387 Reprinted with permission from Ref. (Sun et al., 2022). Copyright 2021, Elsevier. (D) Preparation of

388 four AIE-CDs and their AIE properties at different concentrations. Reprinted with permission from Ref.
389 (Yang et al., 2022). Copyright 2022, Elsevier. (E) Excitation emission spectra of G-NSCDs and
390 B-NSCDs, and schematic diagram of luminescence behavior regulated by the concentration of NSCDs.
391 Reprinted with permission from Ref. (Tang et al., 2023). Copyright 2023, Elsevier. (F) Preparation of
392 N-CDs and quantum yield of CDs. Reprinted with permission from Ref. (Fan et al., 2023). Copyright
393 2023, MDPI.

394

395 **4.2 Analyte concentrations**

396 By controlling the reactant ratio, it is possible to adjust the number of functional
397 groups, the content of heteroatoms, and the degree of carbonization of CDs' surfaces
398 (Su et al., 2020; Yang et al., 2022). Wang et al. prepared four kinds of fluorescent
399 CDs using crystal violet and sulfuric acid solution as precursor and solvent,
400 respectively (Yang et al., 2022). The different content of sulfuric acid solvent will
401 affect the degree of carbonization of CDs to prepare different fluorescent colors of
402 CDs. Sulfuric acid causes intermolecular and intramolecular oxidation dehydration to
403 form large molecular compounds, and the emission wavelength is also redshifted. In
404 their work, Wang et al. showed that by adjusting the solvent concentration,
405 temperature, and reaction time, the luminous wavelength can be controlled, thus
406 enabling applications in fields such as anticounterfeiting and cell imaging. The
407 concentration of the analyte affects the emission wavelength of the CDs (**Fig. 5D**).
408 The preparation of multicolor fluorescent CDs by controlling the fluorescence enables
409 a new kind of fluorescent material with great potential (Cao et al., 2022a; Li and
410 Gong, 2022; Yan et al., 2023). Chen et al. found that nitrogen-sulfur co-doped carbon
411 dots (NSCDs) have green fluorescence at high concentrations (0.2 mg mL^{-1}) and blue

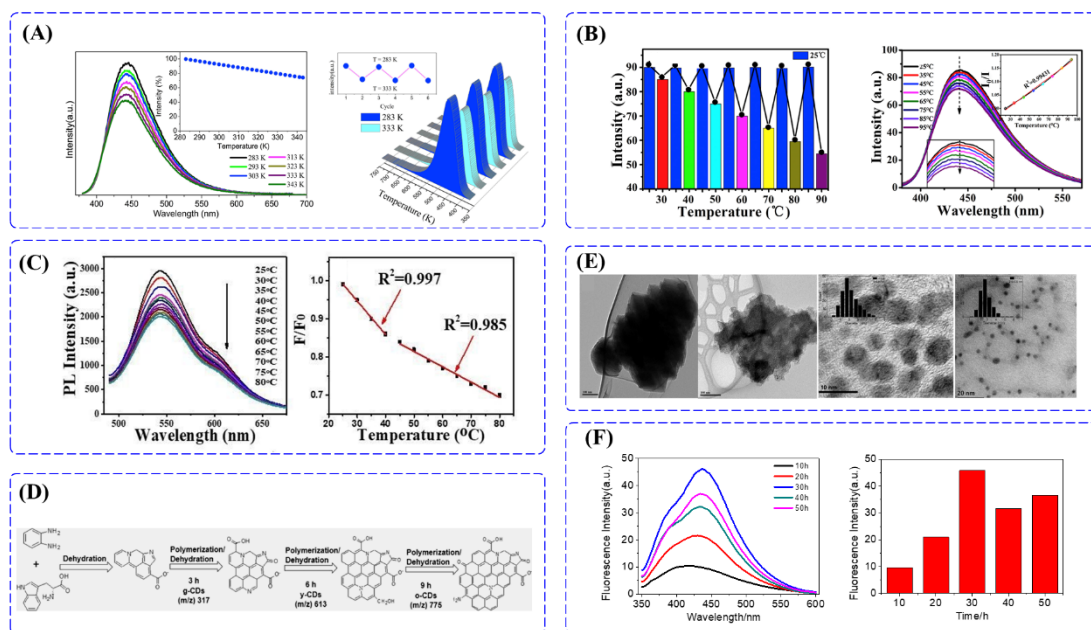
412 fluorescence at low concentrations (0.01 mg mL^{-1}) (Tang et al., 2023). It was further
413 found that the detection behavior was also different under different concentrations
414 (**Fig. 5E**). Fan et al. prepared nitrogen-doped carbon dots (N-CDs) using
415 microcrystalline cellulose (MCC) and PEI as carbon and nitrogen sources (Fan et al.,
416 2023). It was found that the ratio of MCC to PEI is an important factor affecting the
417 fluorescence quantum yield of N-CDs. N-CDs with an MCC/PEI ratio of 1:1 have the
418 highest quantum yield, and the N-CDs can selectively detect Fe^{3+} . (**Fig. 5F**).

419

420 **4.3 Temperature**

421 The fluorescence intensity or emission wavelength of CDs are affected by the
422 temperature (Guo et al., 2020; Zhu et al., 2021). Zhang et al. prepared Cys-CDs with
423 L-cysteine (Cys) and trisodium citrate dihydrate as raw materials, which showed a
424 linear response of fluorescence intensity in the range of 10-70 °C (Guo et al., 2020).
425 The fluorescence intensity decreases when the temperature rises and recovers when
426 the temperature falls again. Quenching is attributed to the activation of nonradiative
427 relaxation channels. Importantly, the light-emitting thermometer made by Cys-CDs
428 can be reused (**Fig. 6A**). The fluorescence intensity of CDs prepared by Guan et al. is
429 reversible at 25-95 °C (Zhang et al., 2020). The CDs use N-aminoethyl piperazine and
430 citric acid as precursors. The reason for the decrease in fluorescence intensity with the
431 increase in temperature is aggregation or the synergistic effect between
432 oxygen-containing functional groups and hydrogen bonds. As a temperature sensor, it
433 has the advantages of a wide response range and high sensitivity (**Fig. 6B**). The

434 yellow, fluorescent CDs prepared by Shai et al. using the hydrothermal method can be
 435 used to detect temperature (Chang et al., 2020). The fluorescence intensity varies with
 436 temperature and has a good linear relationship in the range of 25-40 °C and 45-80 °C.
 437 The excellent response of CDs to temperature makes them suitable for use in
 438 temperature sensors (**Fig. 6C**).



439
 440 **Figure 6.** (A) Fluorescence spectra and temperature reversibility of Cys-CDs solution at different
 441 temperatures. Reprinted with permission from Ref. (Guo et al., 2020). Copyright 2019, Elsevier. (B)
 442 Temperature cycle test of CDs and emission spectra at different temperatures. Reprinted with
 443 permission from Ref. (Zhang et al., 2020). Copyright 2019, Elsevier. (C) γ -CDs luminous intensity at
 444 different temperatures, and linearity of response between F/F_0 and temperature. Reprinted with
 445 permission from Ref. (Chang et al., 2020). Copyright 2020, the Royal Society of Chemistry. (D)
 446 Schematic diagram of MCDs formation. Reprinted with permission from Ref. (Shen et al., 2023).
 447 Copyright 2023, American Chemical Society. (E) TEM images and size distribution of CDs
 448 synthesized at different reaction times. Reprinted with permission from Ref. (Papaioannou et al., 2019).
 449 Copyright 2019, American Chemical Society. (F) Fluorescence spectra and histograms of Phe-CDs at

450 different reaction times. Reprinted with permission from Ref. (Pu et al., 2020). Copyright 2019,
451 Elsevier.

452

453 **4.4 Reaction time**

454 In the synthesis process, the reaction time affects the fluorescence intensity and
455 emission wavelength position of the fluorescent substance. Xu et al. synthesized
456 multicolor CDs using o-phenylenediamine and L-tryptophan as precursors (Shen et al.,
457 2023). With the increase in reaction time, the degree of graphitization and surface
458 state changes. In this system, CDs form small sp^2 domains at 3 h. At 6 h, more
459 precursors participated, and the CD sizes expanded. After 9 h, the CDs surface has
460 extensive conjugated length. The blue, yellow, and orange CDs were prepared by
461 controlling the reaction time, indicating that the reaction time plays an important role
462 in the fluorescence of CDs (**Fig. 6D**). In the work of Titirici et al., CDs were
463 synthesized from glucose by hydrothermal method (Papaioannou et al., 2019). Over
464 the 2-12 h duration of the reaction process, the particle size decreases, and the
465 crystallinity increases. In addition, the different reaction time also affects the intensity
466 of fluorescence. CDs did not show fluorescence after a 2 h reaction. The generation of
467 CDs fluorescence after 4 h could possibly be ascribed to the molecular fluorophore
468 binding on the particle surface or embedding in the amorphous matrix (**Fig. 6E**). Ling
469 et al. prepared CDs from phenylalanine and citric acid with blue fluorescence (Pu et
470 al., 2020). The reaction time also has a certain effect on the fluorescence intensity of
471 CDs. The luminous intensity of CDs increased gradually and reached the maximum at
472 30 h. The results showed that the fluorescence intensity of CDs was related to the

473 reaction time (**Fig. 6F**). Take hydrothermal method as an example: its temperature is
474 roughly 180-200 °C, and the time is 2-12 h. Carbonization at lower temperatures may
475 require an increased reaction time, which can be shortened with the help of
476 microwave-assisted synthesis (Ng et al., 2021). To obtain CDs with excellent
477 performance, it is necessary to optimize the reaction time.

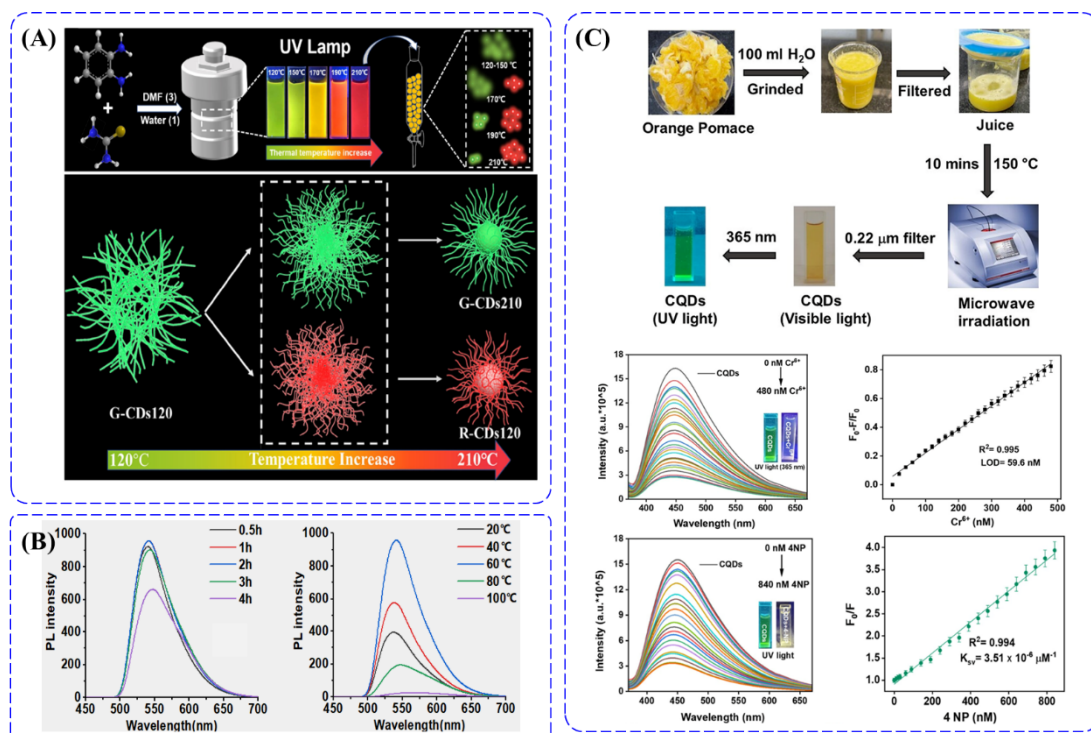
478

479 **5. Improvements in CDs fluorescent sensing**

480 **5.1 Reaction condition optimization**

481 CDs can be prepared by solvothermal method, with carbon source and solvent
482 heated at high temperatures in an autoclave. The preparation process is convenient to
483 operate, and the equipment is cheap (Hu et al., 2016; Kang et al., 2020). The
484 fluorescence properties of CDs prepared at low temperatures are determined by the
485 chromophore, whereas those at high temperatures are determined by the state of the
486 carbonized core (Gao et al., 2021). Fan et al. prepared CDs using a solvothermal
487 method with o-phenylenediamine and thiourea (Gao et al., 2021). Green emission
488 CDs can be separated at relatively low temperatures, and green emission and red
489 emission can be separated at temperatures higher than 170 °C; high-temperature
490 conditions make the fluorescence redshift. The reason for the red emission
491 fluorescence characteristic produced at high temperatures is the polymer property,
492 consisting of carbon core and intertwined polymer chains (**Fig. 7A**). However, the
493 low-temperature CDs synthesis process is more consistent with the concept of green
494 chemistry. Zhao et al. synthesized N,P co-doped CDs at low temperature (Zhao et al.,

2021). The preparation condition of N,P co-doped CDs is only 60 °C, and the synthesis process takes only half an hour. In this synthetic system, the increase of temperature also causes the emission wavelength to redshift, whereas the fluorescence intensity decreases when the temperature exceeds 60 °C (**Fig. 7B**). The low temperature and short duration synthesis process of this system is closer to the concept of green chemistry. Compared with the high-temperature and long-duration CD synthesis process, the method of low-temperature CDs synthesis has more advantages. In the preparation process, the degree of carbonization of CDs is regulated by controlling temperature and time to obtain CDs with high quantum yield. Maity et al. used orange pomace to prepare CQDs by microwave technology (Kundu et al., 2023). During the preparation process, the filtered juice was heated in a microwave reactor for 10 minutes at 150°C (300 W), and the impurities were filtered out to obtain brown CQDs (**Fig. 7C**). The synthesized CQDs have good detection effect on Cr⁶⁺ and 4-NP. Microwave-assisted synthesis is a simple and convenient method, whose reaction time can reach the order of minutes. In addition, to obtain high-quantum-yield CDs, bright and efficient fluorescent chromophores can also be introduced in the synthesis process, or CDs with uniform particle size prepared by template method (Zhang and Lu, 2023).



513

514 **Figure 7.** (A) Schematic diagram of preparation and possible growth mechanism of multicolor
 515 emission CDs. Reprinted with permission from Ref. (Gao et al., 2021). Copyright 2021, Elsevier. (B)
 516 Spectra of N,P-CDs at different reaction times and temperatures. Reprinted with permission from Ref.
 517 (Zhao et al., 2021). Copyright 2020, Elsevier. (C) Preparation and application of CQDs. Reprinted with
 518 permission from Ref. (Kundu et al., 2023). Copyright 2023, American Chemical Society.

519

520 5.2 Sustainable carbon sources

521 There are many kinds of CDs synthesis methods, and the production of CDs
 522 from green biomass materials is receiving increasing attention (Liu et al., 2019a).
 523 When using other carbon sources or nitrogen and sulfur doping to prepare CDs, it is
 524 difficult to avoid the shortcomings of expensive precursors and high costs. Fu et al.
 525 prepared thioctic acid-carbon dots (SCDs) using DL-thioctic acid as a sulfur source

526 and used SCDs as a probe to detect Hg^{2+} and thiophanate methyl (TM) (Wang et al.,
527 2021a). The addition of Hg^{2+} can quench the fluorescence of SCDs at 438 nm, and
528 TM can gradually restore the quenched fluorescence. The reason for quenching is the
529 formation of a complex by static quenching, and the fluorescence recovery is the
530 formation of a complex by TM and Hg^{2+} , which destroys the original structure.
531 Biomass materials such as yeast powder (Cao et al., 2022b), rice fried codonopsis
532 pilosula (Qiu et al., 2020), and cow milk (Kumar et al., 2022) can also be used as
533 carbon sources to prepare CDs. Atchudan et al. used kiwifruit peel as a precursor to
534 prepare CDs for Fe^{3+} detection (Atchudan et al., 2021). As a biomass material, kiwi
535 fruit has rich functional groups. The use of chemicals can be reduced using plant
536 materials. The CDs can be used as a sensor to detect metal ions in the human body or
537 environment and have good selectivity and sensitivity. Li et al. prepared CDs from
538 flax straw, which can be used for the detection of Co^{2+} , Cr^{6+} , and ascorbic acid (Hu et
539 al., 2020). Flax straw contains cellulose, hemicellulose, and lignin, which is a good
540 choice for preparing CDs. Cellulose is a promising sensing material because of its
541 high mechanical strength and good degradation (Ma et al., 2023). The use of these
542 biomass materials not only reduces the use of expensive and some toxic chemical
543 reagents, but it also makes these materials reusable and more environmentally
544 friendly.

545

546 **5.3 Element doping strategy**

547 CDs can be multifunctional by doping with heteroatoms (Guo et al., 2021).
548 Doping of heteroatoms can adjust the optical properties or surface properties of CDs
549 (Zhang et al., 2014). They can be doped with N (Ghafarloo et al., 2020; Latha et al.,
550 2020; Zhi et al., 2022), P (Zhao et al., 2021), Cu (Guo et al., 2021), Fe (Alqahtani et
551 al., 2023), S (Wu et al., 2023), and other heteroatoms (**Table 4**), thus expanding their
552 application in substance detection and other fields. Shuang et al. prepared Cu-doped
553 carbon dots (Cu-CDs) using L-tryptophan and copper chloride as precursors (Guo et
554 al., 2021). By choosing quinine sulfate in water, the quantum yield of Cu-CDs is
555 higher than that of undoped CDs. The fluorescence of Cu-CDs was quenched under
556 the action of tetracycline antibiotics (TCs) based on internal filtration. Due to the
557 doping of Cu on CDs, the strong attraction leads to the formation of Cu-CDs-TCs
558 complexes. Chen et al. used nitrogen-doped CDs (N-CDs) as a probe for the detection
559 of Fe^{3+} (Zhang et al., 2014). Nitrogen doping induces in CDs a strong blue
560 fluorescence and high quantum yield. Importantly, the CDs preparation method is a
561 solid phase thermal strategy, which is simple to operate and can control the transverse
562 size and surface properties of N-CDs. Because of the strong electron affinity of N
563 atoms doped in CDs, the emission wavelength appears as a blue shift compared with
564 N-free CDs. The fluorescence intensity of N-CDs is higher, and the fluorescence
565 lifetime is longer. In addition, Shakir et al. used N and S co-doped CDs (NS CDs) as a
566 probe for the detection of Cr (VI), ascorbic acid and metallic yellow (Abbasi and
567 Shakir, 2022). NS CDs are prepared with mesaconic acid, ethylenediamine, and
568 sulfuric acid as C, N, and S sources. The quantum yield reached 33%. However, the

569 quantum yield of NCDs without sulfuric acid is only 13.8%. Element doping can
 570 adjust the electron energy level structure and chemical properties so that the function
 571 of CDs can be extended (Zhao et al., 2021). To improve the fluorescence sensing of
 572 CDs, the type of reaction solvent can be adjusted to modulate the spectral range
 573 covered by CDs (Liu et al., 2021a; Ran et al., 2023). CDs can also be used with
 574 molecularly imprinted polymers (MIPs) to improve the selectivity and sensitivity of
 575 the sensor (Ansari and Masoum, 2021). In addition, CDs are encapsulated in a porous
 576 material to reduce their accumulation of CDs and achieve an increase in optical
 577 properties (Li et al., 2021a).

578

579 **Table 4.** Heteroatom doping in carbon dots and their analytical performances.

Heteroatom doping	QY (%)		Emission wavelength (nm)		Detector	LOD	Ref.
	(undoped)	(doped)	(undoped)	(doped)			
Cu	2.1	9.5	—	464 (Ex 369)	Tetracyclines , pH	0.16 μ M (Oxytetracycline)	(Guo et al., 2021)
N	9	31	442 (Ex 360)	435 (Ex 360)	Fe^{3+}	2.5 nM	(Zhang et al., 2014)
NS	13.8 (NCDs)	33 (NS CDs)	380 (Ex 320)	405 (Ex 350)	Cr (VI), ascorbic acid, metallic yellow	0.056 μ M; 1 μ M; 0.14 μ M	(Abbasi and Shakir, 2022)

N,P	—	14	—	530 (Ex 430)	antibacterial agent, Sudan Red I	43 nM	(Zhao et al., 2021)
Fe/N	—	33.8	—	440 (Ex 365)	H ₂ O ₂ , glucose	0.36 μM (Glucose, fluorometric)	(Alqahtani et al., 2023)

Ex: excitation wavelength.

580

581 **6. Future perspectives and challenges**

582 Biomass-derived CDs are abundant, inexpensive, non-toxic, and have superior
583 sensing capabilities. The analytical performance of biomass-derived CDs is similar to
584 that of chemical-derived CDs, meaning that they meet the analytical requirements.
585 Using animal derivatives, plants, and household waste as carbon sources can
586 effectively improve the utilization rate of resources. At present, CDs using biomass as
587 raw material have achieved great development. However, how to improve the
588 preparation method and develop these CDs' potential application value is still a
589 challenge. Biomass-derived CDs face the problem of low quantum yield, which needs
590 to be solved by optimizing synthesis methods, element doping, and composite
591 materials. Secondly, the purification of biomass-derived CDs is more challenging.
592 Biomass-derived CDs are diverse and complex in composition, with many functional
593 groups on the surface, and the surface composition and structure are unclear. In the

594 future, greater attention should be focused on purification technologies to treat or
595 reduce by-products. In addition, the production of biomass-derived CDs is low and
596 limited to laboratory research, making it difficult to achieve commercial model
597 production and utilization. Finally, biomass-derived CDs are usually unstable at
598 strong acidity, which limits their application in special environments.

599 Biomass-derived CDs have excellent optical properties and tunable fluorescence
600 characteristics, which can be used as probes for analyte detection, fluorescent ink, and
601 optical devices. CDs have broad application prospects in the manufacturing of
602 light-emitting diodes, luminescent solar concentrators, and other optical devices. The
603 application of CDs in luminescent solar concentrators lays a foundation for their
604 practical application in the future. Their advantages such as low toxicity and good
605 biocompatibility also expand the application of CDs in the biomedical field. In
606 addition, CDs can be used in photocatalysis, electrode materials, room temperature
607 phosphorescence materials, and in other fields. Given the development of the
608 preparation and mechanism of CDs, their potential applications are expected to be
609 extensive.

610

611 **7. Conclusions**

612 In this paper, various factors affecting the fluorescence detection performance of
613 CDs are introduced, and the improvement of their preparation technology as a
614 fluorescence sensing material is briefly described. Results have shown that the
615 reactant concentration, reaction time, reaction temperature, and pH would affect the

616 application of CDs in fluorescence detection. New preparation technology, element
617 doping, and other means can be used to expand its application prospects in different
618 fields. In the fluorescence detection mechanism, the principle of aggregation-induced
619 luminescence and the static quenching mechanism are briefly described. In addition,
620 this paper introduces biomass material as a carbon source. Using plants, animal
621 remains, and microorganisms as raw materials can not only reduce the preparation
622 cost of CDs, but it can also increase the utilization efficiency of resources. The
623 emergence of biomass-derived CDs enables researchers to discover many new
624 possibilities: their excellent properties give them potential application value in
625 fluorescence sensing, fluorescence ink, optical devices, biomedicine, photocatalysis,
626 and other fields. A principal goal of this summary and review of biomass CDs is to
627 stimulate further discussion and application in wider fields.

628

629 **CRedit authorship contribution statement**

630 **Lili Yuan:** Writing – original draft, Writing - review & editing, Conceptualization.

631 **Congying Shao:** Writing – original draft, Writing - review & editing. **Qian Zhang:** Writing –
632 original draft, Writing - review & editing. **Erin Webb:** Writing - review & editing. **Xianhui**

633 **Zhao:** Writing - review & editing. **Shun Lu:** Writing – original draft, Writing - review &
634 editing, Conceptualization, Supervision.

635

636 **Declaration of Competing Interest**

637 The authors declare that they have no known competing financial interests.

638

639 **Data availability**

640 No data was used for the research described in the article.

641

642 **Acknowledgements**

643 This work is supported by the National Natural Science Foundation of China (no.
644 52200076), Natural Science Foundation of Chongqing (grant no.
645 CSTB2022NSCQ-BHX0035), Special Research Assistant Program of Chinese Academy of
646 Science (grant no. 804), Natural Science Foundation of Anhui Province (no. 1708085QB44),
647 University Outstanding Young Talents Program of Anhui province (no. GXYQ2019168), and
648 Research and development of novel fluorescent nanomaterials (no. 22100191). Additionally,
649 this manuscript was authored in part by UT-Battelle LLC under contract
650 DE-AC05-00OR22725 with DOE. The US government retains and the publisher, by
651 accepting the article for publication, acknowledges that the US government retains a
652 nonexclusive, paid-up, irrevocable, worldwide license to publish or reproduce the published
653 form of this manuscript, or allow others to do so, for US government purposes. DOE will
654 provide public access to these results of federally sponsored research in accordance with the
655 DOE Public Access Plan. (<https://www.energy.gov/doe-public-access-plan>).

656

657 **References**

- 658 Abbas, A., et al., 2018. Biomass-waste derived graphene quantum dots and their applications.
659 Carbon. 140, 77-99.
- 660 Abbasi, A., Shakir, M., 2022. Highly crystalline N and S co-doped carbon dots as a selective
661 turn off–on sensor for Cr(VI) and ascorbic acid and a turn off sensor for metanil
662 yellow. Sensors & Diagnostics. 1, 516-524.
- 663 Ai, L., et al., 2021. Insights into photoluminescence mechanisms of carbon dots: advances
664 and perspectives. Sci. Bull. 66, 839-856.
- 665 Alqahtani, Y. S., et al., 2023. Bifunctional nanoprobe for dual-mode detection based on blue
666 emissive iron and nitrogen co-doped carbon dots as a peroxidase-mimic platform.
667 Talanta. 253, 124024.
- 668 Ansari, S., Masoum, S., 2021. Recent advances and future trends on molecularly imprinted
669 polymer-based fluorescence sensors with luminescent carbon dots. Talanta. 223,
670 121411.
- 671 Arumugham, T., et al., 2020. A sustainable synthesis of green carbon quantum dot (CQD)
672 from Catharanthus roseus (white flowering plant) leaves and investigation of its dual
673 fluorescence responsive behavior in multi-ion detection and biological applications.
674 SM&T. 23, e00138.
- 675 Atchudan, R., et al., 2021. Leftover Kiwi Fruit Peel-Derived Carbon Dots as a Highly
676 Selective Fluorescent Sensor for Detection of Ferric Ion. Chemosensors. 9, 166.
- 677 Bei, Y., et al., 2023. Construction of a ratiometric fluorescent probe for visual detection of
678 urea in human urine based on carbon dots prepared from Toona sinensis leaves and
679 5-carboxyfluorescein. Anal. Chim. Acta. 1240, 340733.
- 680 Biswas, M. C., et al., 2021. Graphene Quantum Dots (GQDs) for Bioimaging and Drug
681 Delivery Applications: A Review. ACS Mater. Lett. 3, 889-911.
- 682 Brzechwa-Chodzyńska, A., et al., 2021. Fluorescent sensors: A bright future for cages. Coord
683 Chem Rev. 434 213820.
- 684 Cao, M., et al., 2022a. Ionic Liquid-Assisted Fast Synthesis of Carbon Dots with Strong
685 Fluorescence and Their Tunable Multicolor Emission. Small. 18, 2106683.
- 686 Cao, X., et al., 2022b. Yeast powder derived carbon quantum dots for dopamine detection and
687 living cell imaging. Anal. Methods. 14, 1342-1350.
- 688 Castelletto, S., Boretti, A., 2023. Luminescence solar concentrators: A technology update.
689 Nano Energy. 109, 108269.

690 Castro, R. C., et al., 2021. Visual detection using quantum dots sensing platforms. *Coord*
691 *Chem Rev.* 429, 213637.

692 Chang, D., et al., 2020. Smilax China-derived yellow-fluorescent carbon dots for temperature
693 sensing, Cu²⁺ detection and cell imaging. *Analyst.* 145, 2176-2183.

694 Chen, J., et al., 2021. Recent Progress in Fluorescent Sensors for Drug-Induced Liver Injury
695 Assessment. *ACS Sens.* 6, 628-640.

696 Chen, S., et al., 2018. Inner filter effect-based fluorescent sensing systems: A review. *Anal.*
697 *Chim. Acta.* 999, 13-26.

698 Chen, W., et al., 2022a. Fluorescent probe of nitrogen-doped carbon dots derived from
699 biomass for the sensing of MnO₄⁻ in polluted water based on inner filter effect. *Adv.*
700 *Composites and Hybrid Mater.* 5, 2378-2386.

701 Chen, W., et al., 2022b. Fluorescent probe of nitrogen-doped carbon dots derived from
702 biomass for the sensing of MnO₄⁻ in polluted water based on inner filter effect.
703 *Advanced Composites and Hybrid Materials.* 5, 2378-2386.

704 Das, P., et al., 2020. Carbon Dots for Heavy-Metal Sensing, pH-Sensitive Cargo Delivery,
705 and Antibacterial Applications. *ACS Appl. Nano Mater.* 3, 11777-11790.

706 De Acha, N., et al., 2019. Fluorescent Sensors for the Detection of Heavy Metal Ions in
707 Aqueous Media. *Sensors (Basel).* 19, 599.

708 de Oliveira, B. P., da Silva Abreu, F. O. M., 2021. Carbon quantum dots synthesis from waste
709 and by-products: Perspectives and challenges. *Mater. Lett.* 282, 128764.

710 Deka, M. J., et al., 2022. Recent development of modified fluorescent carbon quantum
711 dots-based fluorescence sensors for food quality assessment. *Carbon Lett.* 32,
712 1131-1149.

713 Deng, Y., et al., 2021. Bio-based electrospun nanofiber as building blocks for a novel
714 eco-friendly air filtration membrane: A review. *Sep. Purif. Technol.* 277, 119623.

715 Dhandapani, E., et al., 2020. Highly green fluorescent carbon quantum dots synthesis via
716 hydrothermal method from fish scale. *Mater. Today: Proc.* 26, A1-A5.

717 Duo, Y., et al., 2023. Biomedical application of aggregation-induced emission
718 luminogen-based fluorescent sensors. *Trends Analyt Chem.* 167, 117252.

719 Fan, J., et al., 2022. Biomass-Derived Carbon Dots and Their Sensing Applications.
720 *Nanomaterials (Basel).* 12, 4473.

721 Fan, J., et al., 2023. Preparation of Microcrystalline Cellulose-Derived Carbon Dots as a
722 Sensor for Fe³⁺ Detection. *Coatings.* 13, 1979.

723 Fang, M., et al., 2024. State-of-the-art of biomass-derived carbon dots: Preparation, properties,
724 and applications. *Chin Chem Lett.* 35, 108423.

725 Feng, Z., et al., 2021. Carbon dot/polymer nanocomposites: From green synthesis to energy,
726 environmental and biomedical applications. *SM&T.* 29, e00304.

727 Fu, L., et al., 2022. A multi-channel array for metal ions discrimination with animal bones
728 derived biomass carbon dots as sensing units. *J. Photoch. Photobio. A.* 424, 113638.

729 Fu, Y., et al., 2021. A carbon dot-based fluorometric probe for oxytetracycline detection
730 utilizing a Förster resonance energy transfer mechanism. *Spectrochim. Acta A Mol.*
731 *Biomol. Spectrosc.* 246, 118947.

732 Gan, J., et al., 2023. Lignocellulosic Biomass-Based Carbon Dots: Synthesis Processes,
733 Properties, and Applications. *Small.* 19, e2304066.

734 Gan, L., et al., 2020. Exploration of pH-responsive carbon dots for detecting nitrite and
735 ascorbic acid. *Appl. Surf. Sci.* 530, 147269.

736 Gao, D., et al., 2021. Temperature triggered high-performance carbon dots with robust
737 solvatochromic effect and self-quenching-resistant deep red solid state fluorescence
738 for specific lipid droplet imaging. *Chem. Eng. J.* 415, 128984.

739 Gao, M., Tang, B. Z., 2017. Fluorescent Sensors Based on Aggregation-Induced Emission:
740 Recent Advances and Perspectives. *ACS Sensors.* 2, 1382-1399.

741 Gao, M., Tang, B. Z., 2020. AIE-based cancer theranostics. *Coord Chem Rev.* 402, 213076.

742 Ghafarloo, A., et al., 2020. Sensitive and selective spectrofluorimetric determination of
743 clonazepam using nitrogen-doped carbon dots. *J. Photochem. Photobiol. A.* 388,
744 112197.

745 Guo, J., et al., 2021. Copper doped carbon dots as the multi-functional fluorescent sensing
746 platform for tetracyclines and pH. *Sens. Actuators B Chem.* 330, 129360.

747 Guo, Z., et al., 2020. A facile synthesis of high-efficient N,S co-doped carbon dots for
748 temperature sensing application. *Dyes Pigm.* 173, 107952.

749 Gupta, D. A., et al., 2020. Fluorescence detection of Fe³⁺ ion using ultra-small fluorescent
750 carbon dots derived from pineapple (*Ananas comosus*): Development of miniaturized
751 analytical method. *J. Mol. Struct.* 1216, 128343.

752 He, Z., et al., 2018. Journey of Aggregation-Induced Emission Research. *ACS Omega.* 3,
753 3267-3277.

754 He, Z., et al., 2023. Recent advances of solvent-engineered carbon dots: A review. *Carbon.*
755 204, 76-93.

756 Horst, F. H., et al., 2021. From cow manure to bioactive carbon dots: a light-up probe for
757 bioimaging investigations, glucose detection and potential immunotherapy agent for
758 melanoma skin cancer. *RSC Adv.* 11, 6346-6352.

759 Hu, G., et al., 2020. Carbon dots derived from flax straw for highly sensitive and selective
760 detections of cobalt, chromium, and ascorbic acid. *J. Colloid Interface Sci.* 579,
761 96-108.

762 Hu, H., et al., 2023. Hour-Level Persistent Multicolor Phosphorescence Enabled by Carbon
763 Dot-Based Nanocomposites Through a Multi-Confinement-Based Approach. *Small.*
764 2308457.

765 Hu, T., et al., 2022. Multifunctional chitosan non-woven fabrics modified with terylene
766 carbon dots for selective detection and efficient adsorption of Cr(VI). *Chem. Eng. J.*
767 432, 134202.

768 Hu, X.-S., et al., 2016. Preparation of flower-like CuS by solvothermal method and its
769 photodegradation and UV protection. *J. Alloys Compd.* 674, 289-294.

770 Huang, Y., et al., 2022a. Novel nitrogen-doped carbon dots for "turn-on" sensing of ATP
771 based on aggregation induced emission enhancement effect. *Spectrochim Acta A Mol*
772 *Biomol Spectrosc.* 273, 121044.

773 Huang, Y., et al., 2022b. Novel nitrogen-doped carbon dots for "turn-on" sensing of ATP
774 based on aggregation induced emission enhancement effect. *Spectrochim. Acta A*
775 *Mol. Biomol. Spectrosc.* 273, 121044.

776 Innocenzi, P., Stagi, L., 2023. Carbon dots as oxidant-antioxidant nanomaterials,
777 understanding the structure-properties relationship. A critical review. *Nano Today.* 50,
778 101837.

779 Jiang, Q., et al., 2020. Potentiality of carbon quantum dots derived from chitin as a
780 fluorescent sensor for detection of ClO⁻. *Microchemical Journal.* 157, 105111.

781 Jing, H. H., et al., 2023. Green Carbon Dots: Synthesis, Characterization, Properties and
782 Biomedical Applications. *J. Funct. Biomater.* 14, 27.

783 Kang, C., et al., 2020. A Review of Carbon Dots Produced from Biomass Wastes.
784 *Nanomaterials (Basel).* 10, 2316.

785 Kang, C., et al., 2022. Aggregation and luminescence in carbonized polymer dots. *Aggregate.*
786 3, e169.

787 Korram, J., et al., 2023. Biomass-Derived Carbon Dots as Nanoprobes for Smartphone–
788 Paper-Based Assay of Iron and Bioimaging Application. ACS Omega. 8,
789 31410-31418.

790 Kousheh, S. A., et al., 2020. Preparation of antimicrobial/ultraviolet protective bacterial
791 nanocellulose film with carbon dots synthesized from lactic acid bacteria. Int. J. Biol.
792 Macromol. 155, 216-225.

793 Kuang, T., et al., 2023. Functional carbon dots derived from biomass and plastic wastes.
794 Green Chem. 25, 6581-6602.

795 Kumar, A., et al., 2022. Synthesis, characterization and potential sensing application of
796 carbon dots synthesized via the hydrothermal treatment of cow milk. Sci. Rep. 12,
797 22495.

798 Kundu, A., et al., 2023. Orange Pomace-Derived Fluorescent Carbon Quantum Dots:
799 Detection of Dual Analytes in the Nanomolar Range. ACS Omega. 8, 22178-22189.

800 Latha, M., et al., 2020. N-doped oxidized carbon dots for methanol sensing in alcoholic
801 beverages. RSC Adv. 10, 22522-22532.

802 Li, B., et al., 2021a. Rational design, synthesis, and applications of carbon dots@metal–
803 organic frameworks (CD@MOF) based sensors. Trends Analyt Chem. 135, 116163.

804 Li, G., et al., 2023a. Recent advancement in graphene quantum dots based fluorescent sensor:
805 Design, construction and bio-medical applications. Coord Chem Rev. 478, 214966.

806 Li, J., Gong, X., 2022. The Emerging Development of Multicolor Carbon Dots. Small. 18,
807 2205099.

808 Li, J., et al., 2023b. Evolution and fabrication of carbon dot-based room temperature
809 phosphorescence materials. Chem. Sci. 14, 3705-3729.

810 Li, J., et al., 2023c. Boosting efficiency of luminescent solar concentrators using ultra-bright
811 carbon dots with large Stokes shift. Nanoscale Horiz. 8, 83-94.

812 Li, L., et al., 2018. Green Synthesis of Multifunctional Carbon Nanodots and Their
813 Applications as a Smart Nanothermometer and Cr(VI) Ions Sensor. Nano. 13,
814 1850147.

815 Li, L., et al., 2021b. Red fluorescent carbon dots for tetracycline antibiotics and pH
816 discrimination from aggregation-induced emission mechanism. Sens. Actuators B
817 Chem. 332, 129513.

818 Li, L., et al., 2021c. Red fluorescent carbon dots for tetracycline antibiotics and pH
819 discrimination from aggregation-induced emission mechanism. *Sensors and*
820 *Actuators B: Chemical*. 332, 129513.

821 Li, S., Zhang, Z., 2021. Recent advances in the construction and analytical applications of
822 carbon dots-based optical nanoassembly. *Talanta*. 223, 121691.

823 Li, X., et al., 2021d. Advances and perspectives in carbon dot-based fluorescent probes:
824 Mechanism, and application. *Coord Chem Rev*. 431, 213686.

825 Liang, H., et al., 2022. Construction of integrated and portable fluorescence sensor and the
826 application for visual detection in situ. *Sens. Actuators B Chem*. 373, 132764.

827 Liao, L., et al., 2023. Highly luminescent nitrogen and sulfur co-doped carbon dots for Sn(2+)
828 and S(2-) sensing and dual-mode anti-counterfeiting. *Mikrochim Acta*. 190, 335.

829 Liao, S., et al., 2021a. Fluorescent nitrogen-doped carbon dots for high selective detecting
830 p-nitrophenol through FRET mechanism. *Spectrochim. Acta A Mol. Biomol.*
831 *Spectrosc*. 259, 119897.

832 Liao, S., et al., 2021b. Fluorescent nitrogen-doped carbon dots for high selective detecting
833 p-nitrophenol through FRET mechanism. *Spectrochim Acta A Mol Biomol Spectrosc*.
834 259, 119897.

835 Liu, G., et al., 2021a. Solvent-controlled synthesis of full-color carbon dots and its application
836 as a fluorescent food-tasting sensor for specific recognition of jujube species. *Sens.*
837 *Actuators B Chem*. 342, 129963.

838 Liu, H., et al., 2020. A novel fluorescence assay based on self-doping biomass carbon dots for
839 rapid detection of dimethoate. *J. Photoch. Photobio. A*. 400, 112724.

840 Liu, H., et al., 2019a. Construction of biomass carbon dots based fluorescence sensors and
841 their applications in chemical and biological analysis. *Trends Analyt Chem*. 118,
842 315-337.

843 Liu, H., et al., 2024. A review of carbon dots in synthesis strategy. *Coord Chem Rev*. 498,
844 215468.

845 Liu, Q., et al., 2019b. Metal-organic framework-based fluorescent sensing of
846 tetracycline-type antibiotics applicable to environmental and food analysis. *Analyst*.
847 144, 1916-1922.

848 Liu, S., et al., 2021b. N,Cl-Codoped Carbon Dots from *Impatiens balsamina* L. Stems and a
849 Deep Eutectic Solvent and Their Applications for Gram-Positive Bacteria

850 Identification, Antibacterial Activity, Cell Imaging, and ClO(-) Sensing. ACS Omega.
851 6, 29022-29036.

852 Luo, X., et al., 2020. Carbon dots derived fluorescent nanosensors as versatile tools for food
853 quality and safety assessment: A review. Trends Food Sci Technol. 95, 149-161.

854 Ma, H., et al., 2023. Advances and challenges of cellulose functional materials in sensors.
855 Journal of Bioresources and Bioproducts. 8, 15-32.

856 Malode, S. J., et al., 2023a. Biomass-derived carbon nanomaterials for sensor applications. J.
857 Pharm. Biomed. Anal. 222, 115102.

858 Malode, S. J., et al., 2023b. Biomass-derived carbon nanomaterials for sensor applications. J
859 Pharm Biomed Anal. 222, 115102.

860 Mathew, S., Mathew, B., 2023a. A review on the synthesis, properties, and applications of
861 biomass derived carbon dots. Inorganic Chemistry Communications. 156, 111223.

862 Mathew, S., Mathew, B., 2023b. A review on the synthesis, properties, and applications of
863 biomass derived carbon dots. Inorg Chem Commun. 156, 111223.

864 Mehta, V. N., et al., 2021. Recent developments on fluorescent hybrid nanomaterials for
865 metal ions sensing and bioimaging applications: A review. J. Mol. Liq. 333, 115950.

866 Meierhofer, F., et al., 2020. Citric Acid Based Carbon Dots with Amine Type Stabilizers:
867 pH-Specific Luminescence and Quantum Yield Characteristics. J. Phys. Chem. C.
868 124, 8894-8904.

869 Meng, W., et al., 2019. Biomass - Derived Carbon Dots and Their Applications. Energy
870 Environ. Mater. 2, 172-192.

871 Meng, Y., et al., 2022. Facile synthesis of multifunctional carbon dots with 54.4% orange
872 emission for label-free detection of morin and endogenous/exogenous hypochlorite. J.
873 Hazard. Mater. 424, 127289.

874 Miao, S., et al., 2020. Hetero-atom-doped carbon dots: Doping strategies, properties and
875 applications. Nano Today. 33, 100879.

876 Mintz, K. J., et al., 2021. A deep investigation into the structure of carbon dots. Carbon. 173,
877 433-447.

878 Ng, H. K. M., et al., 2021. Comparison between hydrothermal and microwave-assisted
879 synthesis of carbon dots from biowaste and chemical for heavy metal detection: A
880 review. Microchem. J. 165, 106116.

881 Niu, G., et al., 2020. AIE luminogens as fluorescent bioprobes. Trends Analyt Chem. 123,
882 115769.

883 Niyitanga, T., et al., 2023. Carbon dots as efficient electrode material for hydrogen peroxide
884 sensing applications: A mini review. *Inorg Chem Commun.* 156, 111249.

885 Oladzadabbasabadi, N., et al., 2023. Turning food waste into value-added carbon dots for
886 sustainable food packaging application: A review. *Adv. Colloid Interface Sci.* 321,
887 103020.

888 Pan, M., et al., 2020. Fluorescent Carbon Quantum Dots—Synthesis, Functionalization and
889 Sensing Application in Food Analysis. *Nanomaterials.* 10, 930.

890 Papaioannou, N., et al., 2019. Investigating the Effect of Reaction Time on Carbon Dot
891 Formation, Structure, and Optical Properties. *ACS Omega.* 4, 21658-21665.

892 Perumal, S., et al., 2021. Sustainable synthesis of multifunctional carbon dots using biomass
893 and their applications: A mini-review. *J. Environ. Chem. Eng.* 9, 105802.

894 Pu, Z. F., et al., 2020. Fluorescent carbon quantum dots synthesized using phenylalanine and
895 citric acid for selective detection of Fe³⁺ ions. *Spectrochim. Acta A Mol. Biomol.*
896 *Spectrosc.* 229, 117944.

897 Qin, K., et al., 2019. Applications of hydrothermal synthesis of Escherichia coli derived
898 carbon dots in in vitro and in vivo imaging and p-nitrophenol detection. *Analyst.* 145,
899 177-183.

900 Qiu, Y., et al., 2020. Facile, green and energy-efficient preparation of fluorescent carbon dots
901 from processed traditional Chinese medicine and their applications for on-site
902 semi-quantitative visual detection of Cr(VI). *Sens. Actuators B Chem.* 324, 128722.

903 Ran, Z., et al., 2023. Multicolor Afterglow from Carbon Dots: Preparation and Mechanism.
904 *Small Methods.* 8, 2301013.

905 Rasal, A. S., et al., 2021. Carbon Quantum Dots for Energy Applications: A Review. *ACS*
906 *Appl. Nano Mater.* 4, 6515-6541.

907 Rasheed, T., 2023. Carbon dots as potential greener and sustainable fluorescent nanomaterials
908 in service of pollutants sensing. *TrAC Trends in Analytical Chemistry.* 158, 116841.

909 Salimi Shahraki, H., et al., 2022. Green carbon dots with multifaceted applications– Waste to
910 wealth strategy. *FlatChem.* 31, 100310.

911 Shan, F., et al., 2021. Novel N-doped carbon dots prepared via citric acid and benzoylurea by
912 green synthesis for high selectivity Fe(III) sensing and imaging in living cells.
913 *Microchem. J.* 167, 106273.

914 Shen, J., et al., 2017. Facile synthesis of fluorescence carbon dots from sweet potato for Fe³⁺
915 sensing and cell imaging. *Mater. Sci. Eng. C.* 76, 856-864.

916 Shen, J., et al., 2023. Reaction Time-Controlled Synthesis of Multicolor Carbon Dots for
917 White Light-Emitting Diodes. *ACS Appl. Nano Mater.* 6, 2478-2490.

918 Shin, Y.-H., et al., 2021. Review—Recent Progress in Portable Fluorescence Sensors. *J.*
919 *Electrochem. Soc.* 168, 017502.

920 Su, Y., et al., 2020. Carbon dots with concentration-modulated fluorescence:
921 Aggregation-induced multicolor emission. *J. Colloid Interface Sci.* 573, 241-249.

922 Sun, L., et al., 2021. Chitosan-derived N-doped carbon dots for fluorescent determination of
923 nitrite and bacteria imaging. *Spectrochim. Acta A Mol. Biomol. Spectrosc.* 251,
924 119468.

925 Sun, X., Lei, Y., 2017. Fluorescent carbon dots and their sensing applications. *Trends Analyt*
926 *Chem.* 89, 163-180.

927 Sun, Z., et al., 2022. High-efficient and pH-sensitive orange luminescence from silicon-doped
928 carbon dots for information encryption and bio-imaging. *J. Colloid Interface Sci.* 607,
929 16-23.

930 Tan, X., et al., 2020a. Signal-on photoluminescent detection of dopamine with carbon
931 dots-MnO₂ nanosheets platform based on inner filter effect. *Dyes and Pigments.* 180,
932 108515.

933 Tan, X., et al., 2020b. Signal-on photoluminescent detection of dopamine with carbon
934 dots-MnO₂ nanosheets platform based on inner filter effect. *Dyes Pigm.* 180, 108515.

935 Tang, X., et al., 2022. Exploration of nitrogen-doped grape peels carbon dots for baicalin
936 detection. *Mater. Today Phys.* 22, 100576.

937 Tang, X., et al., 2021a. Nitrogen-doped fluorescence carbon dots as multi-mechanism
938 detection for iodide and curcumin in biological and food samples. *Bioact. Mater.* 6,
939 1541-1554.

940 Tang, X., et al., 2021b. Nitrogen-doped fluorescence carbon dots as multi-mechanism
941 detection for iodide and curcumin in biological and food samples. *Bioact Mater.* 6,
942 1541-1554.

943 Tang, X., et al., 2023. Concentration-regulated multi-color fluorescent carbon dots for the
944 detection of rifampicin, morin and Al³⁺. *Mater. Today Adv.* 18, 100383.

945 Wang, B., Lu, S., 2022. The light of carbon dots: From mechanism to applications. *Matter.* 5,
946 110-149.

947 Wang, H., et al., 2023a. Aggregation-induced emission (AIE), life and health. *ACS nano.* 17,
948 14347-14405.

949 Wang, H., et al., 2023b. Aggregation-Induced Emission (AIE), Life and Health. ACS Nano.
950 17, 14347-14405.

951 Wang, S., et al., 2021a. A novel thiocetic acid-carbon dots fluorescence sensor for the
952 detection of Hg²⁺ and thiophanate methyl via S-Hg affinity. Food Chem. 346,
953 128923.

954 Wang, S., et al., 2022a. One-pot green synthesis of N,S co-doped biomass carbon dots from
955 natural grapefruit juice for selective sensing of Cr(VI). Chem. Phys. Impact. 5,
956 100112.

957 Wang, X., et al., 2020. Novel mulberry silkworm cocoon-derived carbon dots and their
958 anti-inflammatory properties. Artif Cells Nanomed Biotechnol. 48, 68-76.

959 Wang, Y., et al., 2022b. Synthesis of corn straw-based graphene quantum dots (GQDs) and
960 their application in PO4³⁻ detection. Journal of Environmental Chemical Engineering.
961 10, 107150.

962 Wang, Y., et al., 2021b. Biomass-Derived Carbon Materials: Controllable Preparation and
963 Versatile Applications. Small. 17, 2008079.

964 Wu, L., et al., 2020. Forster resonance energy transfer (FRET)-based small-molecule sensors
965 and imaging agents. Chem. Soc. Rev. 49, 5110-5139.

966 Wu, M., et al., 2023. Design of a Synthetic Strategy to Achieve Enhanced Fluorescent Carbon
967 Dots with Sulfur and Nitrogen Codoping and Its Multifunctional Applications. Small.
968 19, 2302764.

969 Xia, C., et al., 2019. Evolution and Synthesis of Carbon Dots: From Carbon Dots to
970 Carbonized Polymer Dots. Adv. Sci. . 6, 1901316.

971 Yadav, R., et al., 2023. A study on the photophysical properties of strong green-fluorescent
972 N-doped carbon dots and application for pH sensing. Diam Relat Mater. 139, 110411.

973 Yan, F., et al., 2023. Unveiling Unconventional Luminescence Behavior of Multicolor
974 Carbon Dots Derived from Phenylenediamine. J. Phys. Chem. Lett. 14, 5975-5984.

975 Yang, G., et al., 2020. Biodegradable and photostable Nb₂C MXene quantum dots as
976 promising nanofluorophores for metal ions sensing and fluorescence imaging. Sens.
977 Actuators B Chem. 309, 127735.

978 Yang, H., et al., 2018. Carbon dots synthesized by hydrothermal process via sodium citrate
979 and NH₄HCO₃ for sensitive detection of temperature and sunset yellow. J. Colloid
980 Interface Sci. 516, 192-201.

981 Yang, L., et al., 2022. Sulfuric-acid-mediated synthesis strategy for multi-colour
982 aggregation-induced emission fluorescent carbon dots: Application in
983 anti-counterfeiting, information encryption, and rapid cytoplasmic imaging. *J. Colloid*
984 *Interface Sci.* 612, 650-663.

985 Yang, S., et al., 2014. Fluorescence Modulation by Absorbent on Solid Surface: An Improved
986 Approach for Designing Fluorescent Sensor. *Anal. Chem.* 86, 7931-7938.

987 Yin, J., et al., 2021. Small molecule based fluorescent chemosensors for imaging the
988 microenvironment within specific cellular regions. *Chem. Soc. Rev.* 50,
989 12098-12150.

990 Yoo, D., et al., 2019. Carbon Dots as an Effective Fluorescent Sensing Platform for Metal Ion
991 Detection. *Nanoscale Res. Lett.* 14, 272.

992 Zhang, D., et al., 2022a. Red-to-blue colorimetric probe based on biomass carbon dots for
993 smartphone-integrated optosensing of Cu(II) and L-cysteine. *Spectrochim. Acta A*
994 *Mol. Biomol. Spectrosc.* 290, 122285.

995 Zhang, H., et al., 2014. Solid-phase synthesis of highly fluorescent nitrogen-doped carbon
996 dots for sensitive and selective probing ferric ions in living cells. *Anal. Chem.* 86,
997 9846-52.

998 Zhang, H., et al., 2020. Highly luminescent carbon dots as temperature sensors and “off-on”
999 sensing of Hg²⁺ and biothiols. *Dyes Pigm.* 173, 107950.

1000 Zhang, J., et al., 2023a. Recent advances of fluorescent sensors for bacteria detection-A
1001 review. *Talanta.* 254, 124133.

1002 Zhang, L., et al., 2019. Dual-emitting film with cellulose nanocrystal-assisted carbon dots
1003 grafted SrAl₂O₄, Eu²⁺, Dy³⁺ phosphors for temperature sensing. *Carbohydr. Polym.*
1004 206, 767-777.

1005 Zhang, S., et al., 2023b. Kill three birds with one stone: Mitochondria-localized tea saponin
1006 derived carbon dots with AIE properties for stable detection of HSA and extremely
1007 acidic pH. *Food Chem.* 405, 134865.

1008 Zhang, X., et al., 2023c. Chitosan enhanced the stability and antibiofilm activity of
1009 self-propelled Prussian blue micromotor. *Carbohydr Polym.* 299, 120134.

1010 Zhang, Y., Lu, S., 2023. Lasing of carbon dots: Chemical design, mechanisms, and bright
1011 future. *Chem.* 10, 134-171.

1012 Zhang, Y., et al., 2022b. A biomass-derived Schiff base material composited with polylactic
1013 acid nanofiber membrane as selective fluorescent 'turn off/on' platform for Pb²⁺
1014 quantitative detection and characterization. *Int. J. Biol. Macromol.* 214, 414-425.
1015 Zhao, D., et al., 2021. Rapid and low-temperature synthesis of N, P co-doped yellow emitting
1016 carbon dots and their applications as antibacterial agent and detection probe to Sudan
1017 Red I. *Mater. Sci. Eng. C.* 119, 111468.
1018 Zhi, S., et al., 2022. Nitrogen doped carbon dots for sensitive detection of permanganate and
1019 hydrazine by a fluorescence off-on strategy. *Green Anal. Chem.* 3, 100022.
1020 Zhu, J., et al., 2021. Nitrogen and fluorine co-doped green fluorescence carbon dots as a
1021 label-free probe for determination of cytochrome c in serum and temperature sensing.
1022 *J. Colloid Interface Sci.* 586, 683-691.
1023 Zu, F., et al., 2017. The quenching of the fluorescence of carbon dots: A review on
1024 mechanisms and applications. *Microchimica Acta.* 184, 1899-1914.
1025